University of Groningen

Steering Self-Assembly of Amphiphilic Molecular Nanostructures via Halogen Exchange

Kriete, Björn; Bondarenko, Anna; Jumde, Varsha R.; Franken, Linda E.; Minnaard, Adriaan; Jansen, Thomas L. C.; Knoester, Jasper; Pshenitchnikov, Maxim

IMPORTANT NOTE: You are advised to consult the publisher's version (publisher's PDF) if you wish to cite from it. Please check the document version below.

Document Version
Publisher's PDF, also known as Version of record

[Link to publication in University of Groningen/UMCG research database](#)

Letter

Steering Self-Assembly of Amphiphilic Molecular Nanostructures via Halogen Exchange

Björn Kriete,[†,∥] Anna S. Bondarenko,[†,∥] Varsha R. Jumde,[‡,∥] Linda E. Franken,[§] Adriaan J. Minnaard,[‡] Thomas L. C. Jansen,[†] Jasper Knoester,[†] and Maxim S. Pshenichnikov*,[†]

[†]Zernike Institute for Advanced Materials, University of Groningen, Nijenborgh 4, 9747 AG Groningen, The Netherlands
[‡]Stratingh Institute for Chemistry, University of Groningen, Nijenborgh 7, 9747 AG Groningen, The Netherlands
[§]Groningen Biomolecular Sciences and Biotechnology Institute, University of Groningen, Nijenborgh 7, 9747 AG Groningen, The Netherlands

S *Supporting Information*

ABSTRACT: In the field of self-assembly, the quest for gaining control over the supramolecular architecture without affecting the functionality of the individual molecular building blocks is intrinsically challenging. By using a combination of synthetic chemistry, cryogenic transmission electron microscopy, optical absorption measurements, and exciton theory, we demonstrate that halogen exchange in carbocyanine dye molecules allows for fine-tuning the diameter of the self-assembled nanotubes formed by these molecules, while hardly affecting the molecular packing determined by hydrophobic/hydrophilic interactions. Our findings open a unique way to study size effects on the optical properties and exciton dynamics of self-assembled systems under well-controlled conditions.
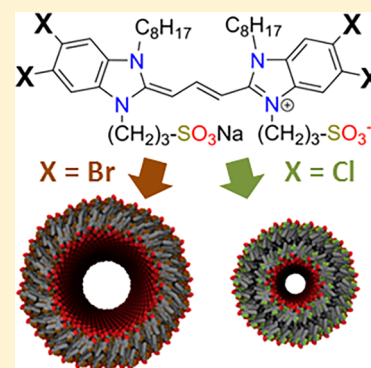
Molecular self-assembly has proven to be a versatile tool in nanotechnology, as it allows for the autonomous and reproducible assembly of a wide variety of low-dimensional functional systems, extending in size from tens of nanometers to microns.[1] A key challenge in the field of self-assembly is to control the shape and size of the final supramolecular structure with minimal changes of the molecular entities that provide the functionality essential for potential applications.[2−4] As the structure of the final assembly is encoded in each individual building block, any modification becomes a highly nontrivial task that requires fine-tuning at the molecular level. It has been shown that tailoring noncovalent molecular interactions such as π-stacking,[5] hydrogen bonding,[6] halogen bonding[7,8] or hydrophobic/hydrophilic interactions[9−11] provides powerful approaches in directing self-assembly. The coordinating nature of hydrophobic/hydrophilic interactions is of special interest, as it may be utilized to tune the supramolecular structure by solely changing the hydrophilic or hydrophobic side groups of the molecules without affecting their functional cores. Indeed, variations of size and composition of the amphiphilic substituents have been used to change between various structures, such as micelles and bilayers, which is often accompanied by changes in the molecular packing.[12,13] In this Letter, we show that even more subtle modifications, namely, just replacing a few halogen atoms, may be used to complement hydrophobic/hydrophilic interactions for fine control over the characteristic size of a self-assembled structure, while preserving the molecules' functional properties and their supramolecular packing.

We demonstrate this control of self-assembly for a class of tubular molecular aggregates of amphiphilic carbocyanine molecules that recently have attracted considerable interest for their optical functionality.[14−16] The close packing of the optically active carbocyanine molecules within the aggregates gives rise to efficient excitation energy transfer and collective optical effects caused by exciton states shared by many molecules.[17] Changing the amphiphilic side groups results in a wide variety of different supramolecular structures,[18−22] of which double-walled tubular structures with a diameter in the order of 10 nm have attracted the most attention.[23−29] The strong interest in these tubular aggregates stems from their structural resemblance to the light-harvesting antennae of photosynthetic green sulfur bacteria,[30−34] which are the most efficient photosynthetic organisms known. Also, the potential of the tubular aggregates as quasi-one-dimensional energy transport wires is of great interest. Previous attempts to control the diameter of tubular aggregates, including changing solvents or adding surfactants yielded only limited variations of the diameter and often completely changed the supramolecular architecture,[35−37] thereby impeding systematic studies of the size effect on the optical functionality and energy transport.
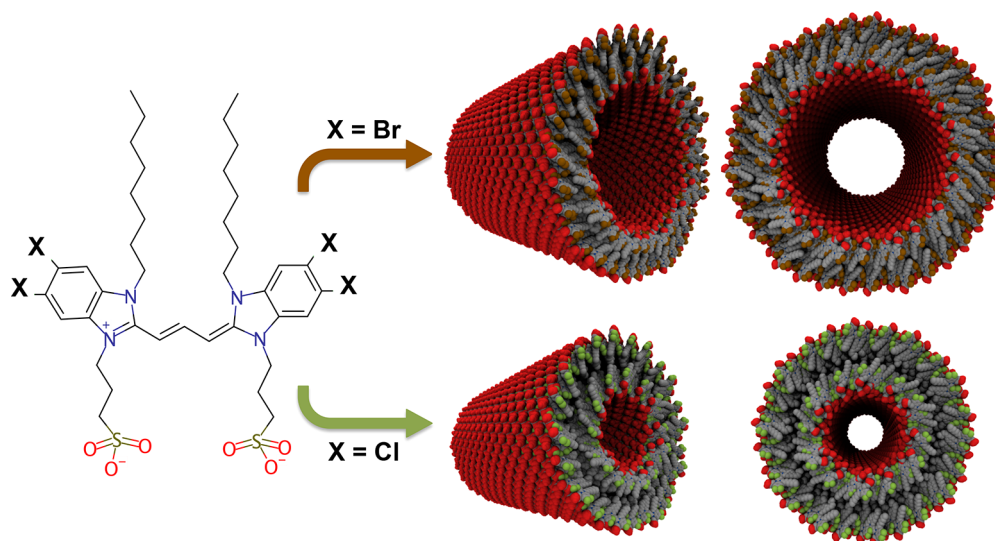
Figure 1. Chemical structure of C8S3. The halogen substituents are abbreviated as X = Br (C8S3-Br) and X = Cl (C8S3-Cl). The right panels illustrate differences in aggregate architectures formed by changing the halogen substituent from chlorine to bromine, as revealed by this work.

In this Letter we show how the diameter of the double-walled tubular system may be increased in a well-defined fashion (by 40% for the outer wall and 110% for the inner one) by replacing the four chlorine atoms in the original carbocyanine molecule by bromine atoms. By measurement and simulation of the absorption spectrum, we show that radial inflation of this tubular system is achieved without significantly altering the molecular packing. Besides extending the toolbox of controlling self-assembly, our results pave the road to greater flexibility in controlling of the diameter of tubular aggregates by, e.g., partial substitution of the halogen atoms. This would provide a model system to elucidate the effects of the inherent structural heterogeneity (namely, variation of the aggregate radii) encountered in natural chlorosomes.[34] Moreover, such systematic control also opens up unprecedented opportunities to study size effects on such important photonics properties as exciton dynamics—a crucial aspect of efficient energy transport—and polarization properties, both equally intriguing from theoretical and experimental points of view.[29,38−40]

The dye molecule of interest in this study is the new cyanine dye derivative 3,3′-bis(2-sulfopropyl)-5,5′,6,6′-tetrabromo-1,1′-dioctylbenzimidacarbocyanine, or C8S3-Br, as opposed to its commercially available and much studied counterpart C8S3-Cl (Figure 1). The new molecules were produced in a four-step synthesis described in detail in the experimental section and the SI.

Exchanging chlorine with bromine slightly shifts the absorption peak of diluted molecules toward longer wavelengths, but introduces no other new features (Figure 2), which is in line with our electronic structure calculations (see Supporting Information (SI)). Addition of Milli-Q water to the methanolic C8S3-Br/Cl stock solutions induces a spectral red-shift of about 75 nm ($\sim$2400 cm^{-1}) and narrowing of absorption and fluorescence bands, both features that are typical for J-type aggregation (Figure 2).

The two sharp low-energy bands that both aggregate spectra have in common are broader for C8S3-Br than for C8S3-Cl. In addition, the high-energy flank of the C8S3-Br aggregate spectrum misses the peaks at $\sim$560 nm and $\sim$570 nm characteristic for the C8S3-Cl aggregate spectrum. Because the optical properties of molecular aggregates are governed by
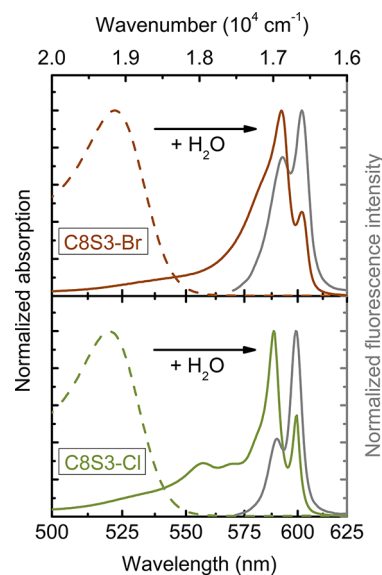

Figure 2. Absorption (solid lines) and fluorescence (solid gray) spectra of molecular aggregates of C8S3-Br (top panel) and C8S3-Cl (bottom panel). Absorption spectra of both molecules diluted in methanol are shown for comparison (dashed lines). For collecting the fluorescence spectra, the excitation wavelength was set to 560 nm.

the interplay of all individual building blocks, the question arises what changes in the aggregate morphology induced by the halogen substitution are responsible for the observed spectral changes.

Experimental evidence for the aggregation of molecules into nanotubes, as schematically depicted in Figure 1, was found by cryo-TEM. Although thicker bundles of C8S3-Br were occasionally observed (see SI), there was no apparent morphological relation with the isolated tubes. Therefore, the more abundant nanotubes will be the focus of this study.

The cryo-TEM micrograph in Figure 3a clearly reveals a double-walled structure of C8S3-Br aggregates, similar to the structure of the C8S3-Cl aggregates (Figure 3b). The profile scans of the aggregates are shown in Figure 3c from which the outer- and inner-wall diameters of C8S3-Br aggregates are
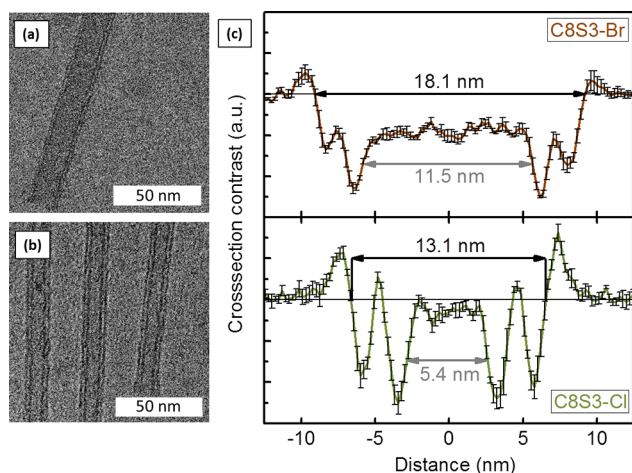
Figure 3. Representative cryo-TEM micrographs for (a) C8S3-Br and (b) C8S3-Cl aggregates illustrate the double-walled structure. (c) Profile scans for C8S3-Br (brown) and C8S3-Cl (green) aggregates, obtained by integrating the signal along the tube axis. The characteristic sizes of the aggregates are indicated by black and gray arrows for the outer and inner cylinder, respectively. The error bars represent the standard error upon averaging individual profile scans. For both C8S3-Cl and C8S3-Br, five straight aggregate segments were used for averaging. The total length over which the profile was integrated amounts to approximately 200 and 400 nm for C8S3-Cl and C8S3-Br, respectively.

obtained as 18.1 ± 0.2 nm and 11.2 ± 0.3 nm, respectively. This is in striking difference with C8S3-Cl aggregates, where these quantities are 13.1 ± 0.2 nm and 5.4 ± 0.1 nm, respectively. Accordingly, the wall-to-wall thickness of C8S3-Br aggregates amounts to 3.4 ± 0.3 nm, which is thinner than for C8S3-Cl aggregates (3.9 ± 0.1 nm). All error margins refer to the standard error upon averaging.

It is important to understand whether the changes in the absorption spectra (Figure 2) are due mainly to the changes in diameter, or whether they result from different molecular packing in both types of aggregates, which results in differences in excitonic interactions. Since the cryo-TEM micrographs lack sufficient signal and 3D analysis to enhance the signal-to-noise ratio requires prior information on the symmetry, we retrieve

the molecular packing by simulating the absorption spectrum for model structures and determining the structural parameters by fitting the experimental spectrum.

As the basic framework, we use the Extended Herringbone (EHB) model, which successfully describes the optical transitions of the double-walled tubular aggregates of C8S3-Cl.[24] Briefly (see SI for more detail), within the EHB model, the molecular positions and orientations are obtained by starting from a rectangular planar lattice of molecules (transition dipoles parallel and in-plane). The molecules are rotated over an angle $\pm\delta$ along their axis (coincident with the transition dipole orientation) and alternately tilted out-of-plane over an angle $\pm\beta$. The lattice is then rolled onto a cylindrical surface over a chiral vector with length equal to the cylinder circumference and direction determined by its angle θ relative to the axis x of the plane (Figure 4). This results in a cylindrical aggregate structure with each unit cell containing two molecules, which in turn leads to four (two Davydov-split) optically dominant exciton transitions per cylinder.[41] The inner and outer cylinders were modeled as spectroscopically independent entities (see sections 4.5 and 6 in the SI for justification), keeping the structural parameters similar for both cylinders, but varying the radii in accordance with the experimental values obtained from cryo-TEM measurements.

The lattice constants of the EHB model were taken to be identical to those for the C8S3-Cl case (see SI), while the free parameters β, δ, and θ that provide the best fit to the measured absorption spectrum for the C8S3-Br aggregate are given in Table 1, along with the original parameters of C8S3-Cl[24] for comparison. Simulation of the absorption spectrum with these structural model parameters indeed gives a good reproduction of the experimental spectrum (Figure 5). In our modeling the lowest-energy peak near 600 nm is associated with the inner wall absorption (in close analogy to C8S3-Cl), while the higher-energy band has contributions from both walls. This spectral assignment of the inner and outer cylinder was verified in oxidation experiments,[24] in which the absorption of the outer cylinder was impaired by silver nanoclusters (see SI). From Table 1, it appears that the molecular packing is essentially preserved upon the Cl → Br exchange, leaving the increase in the radii as the most important factor that changes the

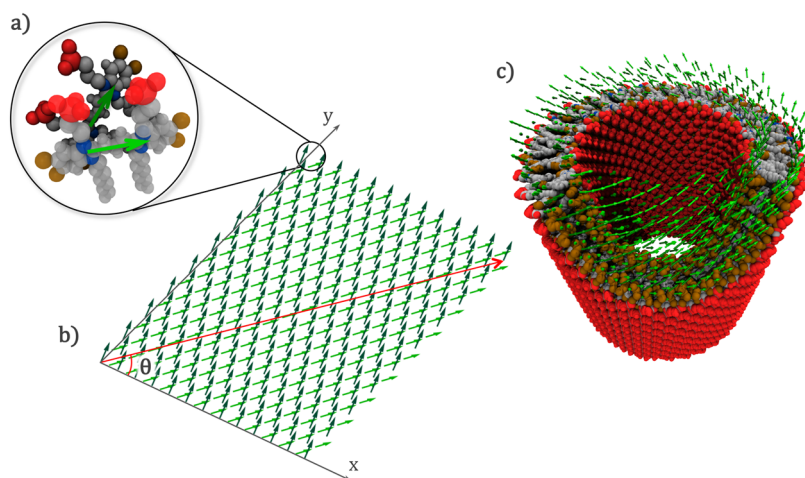**Figure 4.** Schematic representation of the tubular aggregate structure. The molecular pair (a) in each unit cell is shown above the two-dimensional molecular lattice (b). Two lattices are rolled along the chiral vectors (red arrow) to obtain the structure of the double-walled C8S3-Br aggregates shown in panel c, where transition dipole vectors are partially overlapped with the dye molecules.

Table 1. Summary of Structural Model Parameters for the Inner and Outer Walls of C8S3-Br Used in the Calculation of Spectra (Figure 5) Compared to the Model of C8S3-Cl from Ref 24[a]

parameter	C8S3-Br		C8S3-Cl	
	inner cylinder	outer cylinder	inner cylinder	outer cylinder
R/nm	6.50	8.61	3.55	6.47
β/°	23.1	22.3	23.6	23.1
δ/°	25.5	26.0	25.6	28.0
θ/°	55.5	49.4	53.7	53.4

[a]The parameters β and δ define the lattice structure, while the parameter θ defines the aggregate lattice rolling.
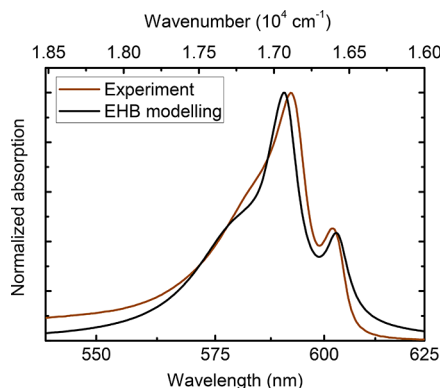

Figure 5. Comparison of the calculated absorption spectrum (black line) and the experimental one (brown line) for the double-walled tubular aggregate of C8S3-Br. The spectra are normalized to their respective peak values.

absorption spectrum, specifically the loss of the high-energy structure. In other words, the observed optical changes arise from an enhanced overlap of the excitonic transitions caused solely by the increase of the tube radius and not by changing the optical properties of the individual dyes or the packing of molecules within the supramolecular assembly.

The modeling of the absorption spectra was performed in the homogeneous limit, i.e., all the molecular transition energies were assumed to be the same. As shown, this suffices to describe the absorption spectra and also explains the polarization properties of the spectral peaks (see SI for linear dichroism), even though in reality some amount of disorder will occur in the transition energies and intermolecular resonance interactions. As has been shown by Bloemsma et al.,[42] in tubular aggregates, such disorder leads to rather weak localization of the excitonic states, which explains the effectiveness of homogeneous models. Allowing for static Gaussian disorder in the transition energies[17,43] and assuming that this disorder solely determines the lowest energy aggregate bandwidth, we find the maximum value (standard deviation) of the disorder to amount to 180 cm^{-1}. More details on the effect of disorder in these aggregates will be published elsewhere.

Above, the large spectral difference between C8S3-Cl and C8S3-Br (Figure 2) was attributed to the change in radii of the inner and outer walls. This interpretation is further substantiated by phenomenologically examining the influence of the cylinder radii on the optical spectra. We modeled 12 cylinders based on the EHB lattice of the inner wall of C8S3-Cl (parameters in Table 1) by only varying the length of the rolling vector resulting in radii from 2.4 to 8.9 nm. For

convenience of comparison (and in contrast to the fit in Figure 5), all spectral transitions were broadened by identical Lorentzian lineshapes of 120 cm^{-1} fwhm. The obtained spectra (Figure 6) reveal congestion of the peaks when going from the
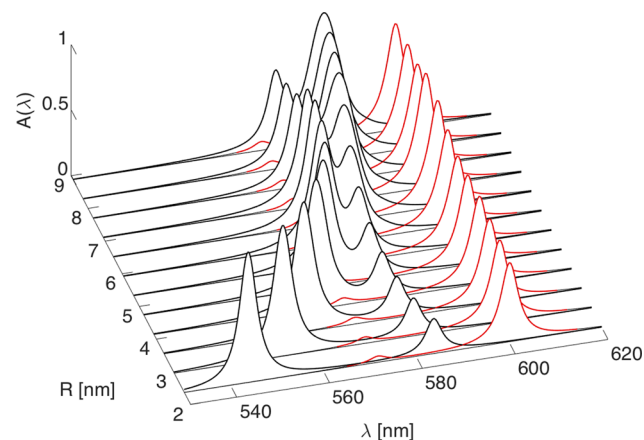

Figure 6. Influence of the tube radius on the absorption spectrum for a single tube with the EHB structure appropriate for the inner wall of C8S3-Cl aggregates. Red and black lines correspond to the spectral components polarized parallel and perpendicular to the tube's axis, respectively. The spectral differences between R = 3.5 nm and R = 6.5 nm reflect the essential differences between the spectra for the inner walls of C8S3-Cl and C8S3-Br.

smallest cylinder with four well separated peaks to the largest cylinder with three peaks with little separation. Two peaks, the large one at 600 nm and the small one at 570 nm, correspond to the doublet of transitions polarized parallel to the tube axis with their positions essentially independent of the radii. With increasing radius, the doublet of peaks with perpendicular polarization moves down in energy toward the parallel peaks, reflecting the fact that upon decreasing the cylinder curvature, the energy separation between corresponding parallel and perpendicular transitions decreases.[15] Consequently, with increasing cylinder radius, high-energy peaks vanish and spectral structure gets lost. In experiment, this effect is further enhanced by a stronger broadening of the higher-energy exciton peaks due to intraband relaxation, an effect not accounted for in Figure 6.

In conclusion, we have shown that a very moderate chemical modification through the exchange of four halogen atoms in the chromophore of an amphiphilic carbocyanine dye leads to well-defined changes in the final supramolecular assembly without altering the underlying molecular architecture. This allowed us to study the effect of purely radial growth on the collective optical properties of the supramolecular structure. In a broader perspective, our results demonstrate that a combination of halogen exchange and amphiphilically driven self-assembly opens up unprecedented opportunities in controlling the supramolecular structure to a fine degree for systems, where modifications of other molecular moieties and/or changes of the immediate environment (solvent, pH, external fields) are not feasible as is the case in, e.g., many biological systems or for medical applications. In addition, we believe that the presented design principle can be transferred to structurally related molecules that are known to form other supramolecular architectures, such as single-walled tubes,[44] twisted bundles[19] or vesicles.[19,35] Nonetheless, the exact underlying mechanism of how halogen exchange affects the aggregation behavior is yet

Scheme 1. Four-Step Synthesis of Compound 5 (C8S3-Br)
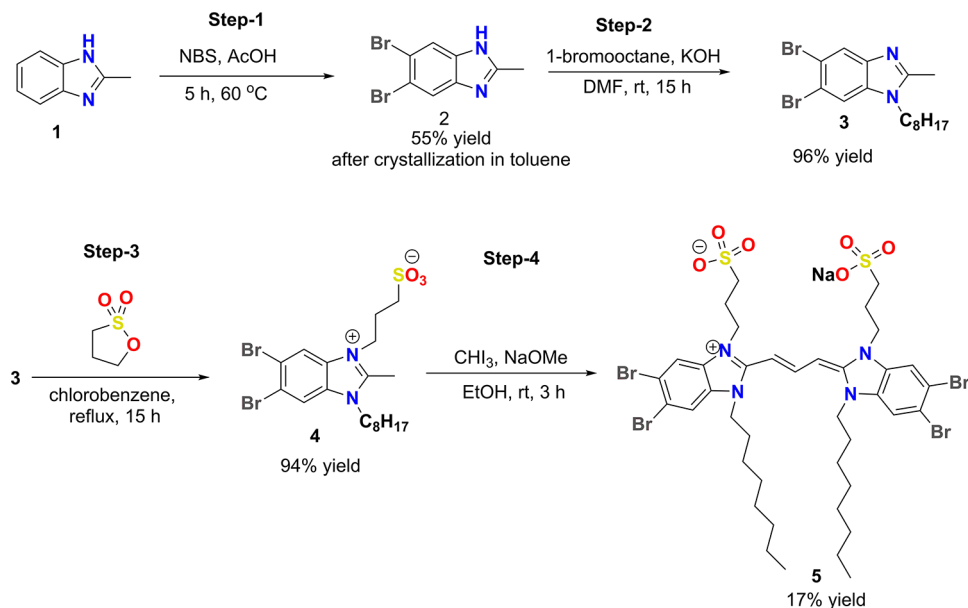
to be understood. Our results suggest that the size of the halogen substituents and/or the ability to form halogen bonds play an important role. For instance, fluorine, unlike bromine or chlorine, is known to hardly form halogen bonds and may even lead to intermolecular repulsion,[8] which would impede the formation of molecular aggregates. We tested this concept experimentally by synthesizing the C8S3-F molecule and indeed found a poor degree of aggregation under normal conditions (see SI). Based on our results, it is envisioned that further studies of partial replacement of only a few halogen atoms will shed light on the effect of different halogen substituents on the aggregation behavior. This would open great prospects for fine-tuning size effects for optical functionality and for optimization of tubular aggregates for specific applications such as, for instance, artificial light-harvesting systems.

■ MATERIALS AND SAMPLE PREPARATION

The dye 3,3′-bis(2-sulfopropyl)-5,5′,6,6′-tetrachloro-1,1′-dioctylbenzimidacarbocyanine (C8S3-Cl, M = 903 g mol^{-1}) was purchased from FEW Chemicals GmbH (Wolfen, Germany) and used as received without further purification. The synthesis and purification of amphiphilic cyanine dye derivative 3,3′-bis(2-sulfopropyl)-5,5′,6,6′-tetrabromo-1,1′-dioctyl-benzimidacarbocyanine (C8S3-Br, M = 1081 g mol^{-1}) involves four steps and is outlined in Scheme 1.

2-Methylbenzimidazole (**1**) was converted into 5,6-dibromo-2-methylbenzimidazole (**2**), by bromination with NBS according to the modified literature procedure.[45] Selective bromination was achieved at the 5 and 6 positions, and pure compound was obtained in 55% yield after crystallization in toluene. The corresponding benzimidazole was then treated with 1-bromooctane in the presence of KOH to obtain 5,6-dibromo-2-methyl-1-octyl-benzimidazole (**3**), in almost quantitative yield after work up.[46,47] The quaternization of **3** with 1,3-propane sultone (step 3, Scheme 1) was carried out according to a reported procedure.[21,22,48] The reaction conditions involved reflux in chlorobenzene at 120−130 °C to obtain the sulfoalkyl substituted dye precursor **4**. The last step consists

of condensation of two equivalents of **4** with iodoform in alkaline medium affording dye **5**.[22] To obtain pure dye, the crude was recrystallized in a DMF water mixture. Additional information including NMR spectra and quantum yield measurements are provided in the SI.

Molecular aggregates of the dyes were prepared via the alcoholic route.[15] The molecules were first dissolved in pure methanol (Biosolve) to form 1.75 mM stock solutions. In the next step, the stock solution was added to Milli-Q water to induce aggregation and render a methanol content of 14 wt % in the final sample solution. An immediate color change from orange to pink was detected by the naked eye, indicating the fast formation of J-aggregates due to hydrophobic solvent interactions. The resulting solution was gently shaken and stored in the dark at room temperature for days up to weeks for aggregation. The final dye concentration in the aggregate solution was 0.236 mM.

Steady State Absorption and Fluorescence Emission. Steady-state UV−vis absorption spectra were measured using a PerkinElmer Lambda 900 UV/vis/NIR spectrometer. For the pristine dyes, diluted versions of the stock solutions were prepared with final dye concentrations in the range of 10^{-4} mol L^{-1}. Prior to measurements, aggregate sample solutions were diluted with Milli-Q water by factor 2. Steady-state fluorescence emission spectra were recorded using a PerkinElmer LS50B Luminescence Spectrometer and 10 mm quartz cuvette (Starna GmbH, Germany). In order to avoid fluorescence reabsorption, aggregate sample solutions were diluted with Milli-Q water by approximately a factor of 100.

Cryogenic Transmission Electron Microscopy. To prepare the samples for cryogenic transmission electron microscopy (cryo-TEM), a 3 μL droplet of the sample solution was placed on a copper grid with holey carbon film (quantifoil 3.5/1), which was first hydrophilized by glow discharging. In order to obtain a thin layer of the solution in the range of 100 nm, the excess fluid was blotted off for 5 s. Immediately afterward, the grid was vitrified in liquid ethane at its freezing point (−184 °C) with a Vitrobot (FEI, Eindhoven, The Netherlands). The grids were placed in a cryotransfer holder (Gatan model 626) and transferred into a Philips CM120 transmission electron

microscope with an LaB6 cathode or a tungsten hairpin cathode operated at 120 kV. Micrographs were recorded with an UltraScan 4000 UHS CCD camera (Gatan, Pleasanton, CA, USA) using low-dose mode.

Theoretical Calculations and Modeling. The geometry of each cylindrical tube of the double-walled tubular aggregate of C8S3-Br was obtained by rolling an EHB lattice with two molecules per unit cell.[24] The construction of the lattice and rolling procedure is briefly described in the main text and in detail in the SI. All the input structural and energetic parameters were obtained either from previous studies[15,49,50] or obtained from the present cryo-TEM and optical experiments.

Optical electronic transitions were obtained by numerical diagonalization of the Frenkel exciton Hamiltonian[17] that accounts for molecular transition energies and Coulomb transfer interactions between the molecules with an extended dipole coupling model.[15,49] Coupling between the walls was neglected, allowing separate calculations for both walls. This approximation[24] is acceptable, as the largest interwall couplings are significantly smaller than the intrawall couplings and smaller than the homogeneous line width (see section 4.5 in the SI). The fitted spectrum was obtained in the homogeneous limit where there is no disorder in the molecular transition energies. The obtained stick spectrum was broadened with Lorentzians of different widths for optimal agreement with the experiment. Details are given in the SI.

ASSOCIATED CONTENT

Ⓢ Supporting Information

The Supporting Information is available free of charge on the ACS Publications website at DOI: 10.1021/acs.jpclett.7b00967.

> Synthesis of C8S3-Br and C8S3-F including NMR spectra, quantum yield of C8S3-Br monomers and aggregates, absorption spectrum and cryo-TEM of C8S3-Br bundles, details of the theoretical modeling including coupling strengths between inner and outer cylinder, linear dichroism spectrum, time-resolved fluorescence of C8S3-Br aggregates, oxidation of aggregation for spectral assignment, and aggregation of C8S3-F. (PDF)

AUTHOR INFORMATION

Corresponding Author

*E-mail: M.S.Pchenitchnikov@rug.nl.

ORCID Ⓘ

Adriaan J. Minnaard: 0000-0002-5966-1300
Thomas L. C. Jansen: 0000-0001-6066-6080
Maxim S. Pshenichnikov: 0000-0002-5446-4287

Author Contributions

‖These authors contributed equally to this work. B.K. performed the aggregate self-assembling and the optical experiments; the analysis was supervised by M.S.P. B.K. and L.E.F. performed the cryo-TEM experiments. A.S.B. performed the theoretical modeling and interpreted the optical spectra supervised by T.L.C.J. and J.K. V.R.J. performed the organic synthesis supervised by A.J.M. T.L.C.J., J.K., and M.S.P. conceived and developed the project. B.K., V.R.J., A.S.B., T.L.C.J., J.K., and M.S.P. wrote the paper.

Notes

The authors declare no competing financial interest.

REFERENCES

(1) Whitesides, G. M.; Grzybowski, B. Self-assembly at all scales. *Science* **2002**, *295*, 2418−2421.

(2) Hickey, R. J.; Koski, J.; Meng, X.; Riggleman, R. A.; Zhang, P.; Park, S.-J. Size-Controlled Self-Assembly of Superparamagnetic Polymersomes. *ACS Nano* **2014**, *8*, 495−502.

(3) Ghoroghchian, P. P.; Frail, P. R.; Susumu, K.; Blessington, D.; Brannan, A. K.; Bates, F. S.; Chance, B.; Hammer, D. A.; Therien, M. J. Near-infrared-emissive polymersomes: self-assembled soft matter for in vivo optical imaging. *Proc. Natl. Acad. Sci. U. S. A.* **2005**, *102*, 2922−2927.

(4) Howse, J. R.; Jones, R. A. L.; Battaglia, G.; Ducker, R. E.; Leggett, G. J.; Ryan, A. J. Templated formation of giant polymer vesicles with controlled size distributions. *Nat. Mater.* **2009**, *8*, 507−511.

(5) Hoeben, F. J. M.; Jonkheijm, P.; Meijer, E. W.; Schenning, A. P. H. J. About Supramolecular Assemblies of π-Conjugated Systems. *Chem. Rev.* **2005**, *105*, 1491−1546.

(6) Kaiser, T. E.; Wang, H.; Stepanenko, V.; Würthner, F. Supramolecular Construction of Fluorescent J-Aggregates Based on Hydrogen-Bonded Perylene Dyes. *Angew. Chem., Int. Ed.* **2007**, *46*, 5541−5544.

(7) Corradi, E.; Meille, S. V.; Messina, M. T.; Metrangolo, P.; Resnati, G. Halogen Bonding versus Hydrogen Bonding in Driving Self-Assembly Processes. *Angew. Chem.* **2000**, *112*, 1852−1856.

(8) Cavallo, G.; Metrangolo, P.; Milani, R.; Pilati, T.; Priimagi, A.; Resnati, G.; Terraneo, G. The Halogen Bond. *Chem. Rev.* **2016**, *116*, 2478−2601.

(9) Wang, C.; Wang, Z.; Zhang, X. Amphiphilic Building Blocks for Self-Assembly: From Amphiphiles to Supra-amphiphiles. *Acc. Chem. Res.* **2012**, *45*, 608−618.

(10) Sadownik, J. W.; Mattia, E.; Nowak, P.; Otto, S. Diversification of self-replicating molecules. *Nat. Chem.* **2016**, *8*, 264−269.

(11) van Dijken, D. J.; Chen, J.; Stuart, M. C. A.; Hou, L.; Feringa, B. L. Amphiphilic Molecular Motors for Responsive Aggregation in Water. *J. Am. Chem. Soc.* **2016**, *138*, 660−669.

(12) Ramanathan, M.; Shrestha, L. K.; Mori, T.; Ji, Q.; Hill, J. P.; Ariga, K. Amphiphile nanoarchitectonics: from basic physical chemistry to advanced applications. *Phys. Chem. Chem. Phys.* **2013**, *15*, 10580−10611.

(13) Du, J.; O'Reilly, R. K. Advances and challenges in smart and functional polymer vesicles. *Soft Matter* **2009**, *5*, 3544−3561.

(14) Spitz, C.; Knoester, J.; Ouart, A.; Daehne, S. Polarized absorption and anomalous temperature dependence of fluorescence depolarization in cylindrical J-aggregates. *Chem. Phys.* **2002**, *275*, 271−284.

(15) Didraga, C.; Pugžlys, A.; Hania, P. R.; von Berlepsch, H.; Duppen, K.; Knoester, J. Structure, spectroscopy, and microscopic model of tubular carbocyanine dye aggregates. *J. Phys. Chem. B* **2004**, *108*, 14976−14985.

(16) Würthner, F.; Kaiser, T. E.; Saha-Möller, C. R. J-Aggregates: From Serendipitous Discovery to Supramolecular Engineering of Functional Dye Materials. *Angew. Chem., Int. Ed.* **2011**, *50*, 3376−3410.

(17) Fidder, H.; Knoester, J.; Wiersma, D. A. Optical properties of disordered molecular aggregates: A numerical study. *J. Chem. Phys.* **1991**, *95*, 7880−7890.

(18) Pawlik, A.; Ouart, A.; Kirstein, S.; Abraham, H.-W.; Dähne, S. Synthesis and UV/Vis Spectra of J-Aggregating 5, 5′, 6, 6′-Tetrachlorobenzimidacarbocyanine Dyes for Artificial Light-Harvesting Systems and for Asymmetrical Generation of Supramolecular Helices. *Eur. J. Org. Chem.* **2003**, *2003*, 3065−3080.

(19) Kirstein, S.; Dähne, S. J-aggregates of amphiphilic cyanine dyes: Self-organization of artificial light harvesting complexes. *Int. J. Photoenergy* **2006**, *2006*, 20363.

(20) von Berlepsch, H.; Ludwig, K.; Kirstein, S.; Böttcher, C. Mixtures of achiral amphiphilic cyanine dyes form helical tubular J-aggregates. *Chem. Phys.* **2011**, *385*, 27−34.

(21) Pawlik, A.; Kirstein, S.; De Rossi, U.; Dähne, S. Structural conditions for spontaneous generation of optical activity in J-aggregates. *J. Phys. Chem. B* **1997**, *101*, 5646−5651.

(22) De Rossi, U.; Moll, J.; Spieles, M.; Bach, G.; Dähne, S.; Kriwanek, J.; Lisk, M. Control of the J-Aggregation Phenomenon by variation of the N-alkyl-substituents. *J. Prakt. Chem./Chem.-Ztg.* **1995**, *337*, 203−208.

(23) Abramavicius, D.; Nemeth, A.; Milota, F.; Sperling, J.; Mukamel, S.; Kauffmann, H. F. Weak exciton scattering in molecular nanotubes revealed by double-quantum two-dimensional electronic spectroscopy. *Phys. Rev. Lett.* **2012**, *108*, 67401.

(24) Eisele, D. M.; Cone, C. W.; Bloemsma, E. A.; Vlaming, S. M.; van der Kwaak, C. G. F.; Silbey, R. J.; Bawendi, M. G.; Knoester, J.; Rabe, J. P.; Vanden Bout, D. A. Vanden. Utilizing redox-chemistry to elucidate the nature of exciton transitions in supramolecular dye nanotubes. *Nat. Chem.* **2012**, *4*, 655−662.

(25) Clark, K. A.; Cone, C. W.; Vanden Bout, D. A. Quantifying the Polarization of Exciton Transitions in Double-Walled Nanotubular J-Aggregates. *J. Phys. Chem. C* **2013**, *117*, 26473−26481.

(26) Eisele, D. M.; Arias, D. H.; Fu, X.; Bloemsma, E. A.; Steiner, C. P.; Jensen, R. A.; Rebentrost, P.; Eisele, H.; Tokmakoff, A.; Lloyd, S.; et al. Robust excitons inhabit soft supramolecular nanotubes. *Proc. Natl. Acad. Sci. U. S. A.* **2014**, *111*, E3367−E3375.

(27) Yuen-Zhou, J.; Arias, D. H.; Eisele, D. M.; Steiner, C. P.; Krich, J. J.; Bawendi, M. G.; Nelson, K. A.; Aspuru-Guzik, A. Coherent exciton dynamics in supramolecular light-harvesting nanotubes revealed by ultrafast quantum process tomography. *ACS Nano* **2014**, *8*, 5527−5534.

(28) Megow, J.; Röhr, M. I. S.; Schmidt am Busch, M.; Renger, T.; Mitrić, R.; Kirstein, S.; Rabe, J. P.; May, V.; et al. Site-dependence of van der Waals interaction explains exciton spectra of double-walled tubular J-aggregates. *Phys. Chem. Chem. Phys.* **2015**, *17*, 6741−6741.

(29) Caram, J. R.; Doria, S.; Eisele, D. M.; Freyria, F. S.; Sinclair, T. S.; Rebentrost, P.; Lloyd, S.; Bawendi, M. G. Room-Temperature Micron-Scale Exciton Migration in a Stabilized Emissive Molecular Aggregate. *Nano Lett.* **2016**, *16*, 6808−6815.

(30) Cogdell, R. J.; Gardiner, A. T.; Hashimoto, H.; Brotosudarmo, T. H. P. A comparative look at the first few milliseconds of the light reactions of photosynthesis. *Photochem. Photobiol. Sci.* **2008**, *7*, 1150−1158.

(31) Ganapathy, S.; Oostergetel, G. T.; Wawrzyniak, P. K.; Reus, M.; Chew, A. G. M.; Buda, F.; Boekema, E. J.; Bryant, D. A.; Holzwarth, A. R.; de Groot, H. J. M. Alternating syn-anti bacteriochlorophylls form concentric helical nanotubes in chlorosomes. *Proc. Natl. Acad. Sci. U. S. A.* **2009**, *106*, 8525−8530.

(32) McConnell, I.; Li, G.; Brudvig, G. W. Energy conversion in natural and artificial photosynthesis. *Chem. Biol.* **2010**, *17*, 434−447.

(33) Orf, G. S.; Blankenship, R. E. Chlorosome antenna complexes from green photosynthetic bacteria. *Photosynth. Res.* **2013**, *116*, 315−331.

(34) Günther, L. M.; Jendrny, M.; Bloemsma, E. A.; Tank, M.; Oostergetel, G. T.; Bryant, D. A.; Knoester, J.; Köhler, J. Structure of Light-Harvesting Aggregates in Individual Chlorosomes. *J. Phys. Chem. B* **2016**, *120*, 5367−5376.

(35) von Berlepsch, H.; Kirstein, S.; Hania, R.; Pugzlys, A.; Böttcher, C. Modification of the nanoscale structure of the J-aggregate of a sulfonate-substituted amphiphilic carbocyanine dye through incorpo-ration of surface-active additives. *J. Phys. Chem. B* **2007**, *111*, 1701−1711.

(36) von Berlepsch, H.; Kirstein, S.; Böttcher, C. Effect of alcohols on J-aggregation of a carbocyanine dye. *Langmuir* **2002**, *18*, 7699−7705.

(37) von Berlepsch, H.; Kirstein, S.; Böttcher, C. Supramolecular structure of J-aggregates of a sulfonate substituted amphiphilic carbocyanine dye in solution: Methanol-induced ribbon-to-tubule transformation. *J. Phys. Chem. B* **2004**, *108*, 18725−18733.

(38) Vlaming, S. M.; Bloemsma, E. A.; Nietiadi, M. L.; Knoester, J. Disorder-induced exciton localization and violation of optical selection rules in supramolecular nanotubes. *J. Chem. Phys.* **2011**, *134*, 114507.

(39) Clark, K. A.; Krueger, E. L.; Vanden Bout, D. A. Direct measurement of energy migration in supramolecular carbocyanine dye nanotubes. *J. Phys. Chem. Lett.* **2014**, *5*, 2274−2282.

(40) Chuang, C.; Lee, C. K.; Moix, J. M.; Knoester, J.; Cao, J. Quantum Diffusion on Molecular Tubes: Universal Scaling of the 1D to 2D Transition. *Phys. Rev. Lett.* **2016**, *116*, 196803.

(41) Didraga, C.; Klugkist, J. A.; Knoester, J. Optical Properties of Helical Cylindrical Molecular Aggregates: The Homogeneous Limit. *J. Phys. Chem. B* **2002**, *106*, 11474.

(42) Bloemsma, E. A.; Vlaming, S. M.; Malyshev, V. A.; Knoester, J. Signature of Anomalous Exciton Localization in the Optical Response of Self-Assembled Organic Nanotubes. *Phys. Rev. Lett.* **2015**, *114*, 156804.

(43) Didraga, C.; Knoester, J. Optical spectra and localization of excitons in inhomogeneous helical cylindrical aggregates. *J. Chem. Phys.* **2004**, *121*, 10687−10698.

(44) Friedl, C.; Renger, T.; Berlepsch, H. v.; Ludwig, K.; Schmidt am Busch, M.; Megow, J. Structure Prediction of Self-Assembled Dye Aggregates from Cryogenic Transmission Electron Microscopy, Molecular Mechanics, and Theory of Optical Spectra. *J. Phys. Chem. C* **2016**, *120*, 19416−19433.

(45) El Kihel, A.; Benchidmi, M.; Essassi, E. M.; Danion-Bougot, R. Halogenation of Substituted Benzimidazoles. Nitration of the Resulting Halobenzimidazoles. *Synth. Commun.* **1999**, *29*, 387−397.

(46) Kikugawa, Y. A Facile N-Alkylation of Imidazoles and Benzimidazoles. *Synthesis* **1981**, *1981*, 124−125.

(47) Kyrides, L. P.; Zienty, F. B.; Steahly, G. W.; Morrill, H. L. Substituted Imidazoles and Benzimidazoles. *J. Org. Chem.* **1947**, *12*, 577−586.

(48) Wolfbeis, O. S.; Urbano, E. Syntheses of fluorescent dyes. XIV. Standards for fluorescence measurements in the near neutral pH-range. *J. Heterocycl. Chem.* **1982**, *19*, 841−843.

(49) Czikkely, V.; Försterling, H. D.; Kuhn, H. Light absorption and structure of aggregates of dye molecules. *Chem. Phys. Lett.* **1970**, *6*, 11−14.

(50) Jorgensen, W. L.; Severance, D. L. Aromatic-aromatic interactions: free energy profiles for the benzene dimer in water, chloroform, and liquid benzene. *J. Am. Chem. Soc.* **1990**, *112*, 4768−4774.